IEEE 15th International Workshop on Advanced Motion Control
March 9-11, 2018, Tokyo, Japan

Accepted article

Design and Analysis of non-linear Circuit with Tunnel Diode for Hybrid Control Systems

Philipp Pasolli
University of Agder (UiA)
Faculty of Engineering and Science
Post box 422, 4604-Kristiansand, Norway
philipp.pasolli@uia.no

Michael Ruderman
University of Agder (UiA)
Faculty of Engineering and Science
Post box 422, 4604-Kristiansand, Norway
michael.ruderman@uia.no

***Abstract*—Electric circuits with tunnel diode's represent a classical example of dynamic systems with nonlinearities, which feature piecewise negative damping and multiple equilibria and, as consequence, nontrivial trajectories in the state-space. In this paper, we describe the experimental design and analysis of an electrical circuit, including a tunnel diode, allowing for a storage behavior with bistable output voltage states – *low* and *high*. The system is modeled for simulation and an experimental setup is designed and implemented in order to run a formal verification on different tools, applying a variety of hybrid control methods. The nonlinear diode's characteristic curve is experimentally determined and evaluated. The transient response of circuit is also analyzed. Furthermore the circuit is controlled in an open loop manner, by a biased sequence of pulse signals, showing a bistable switching behavior of the output voltage state.**

***Index Terms*—tunnel diode, nonlinearity, electric circuits, hybrid control, system analysis, bistable behavior**

I. Introduction

Since invented and introduced, the tunnel diodes belong to standard electronic elements, which can be used for a wide variety of functions such as amplifying, switching, frequency conversion, etc [7]. Formerly used in microwave oscillators [13], tunnel diodes have entered diversity of semiconductor technologies and micro-electronics applications, like for example in computer memory, but also in various other logic circuits, see e.g. [2]. Even though representing a well-understood and widely established semiconductor technology, the tunneling diodes remain further in focus of investigation in conjunction with unique current-voltage characteristics and associated properties of nonlinear electric circuits. For instance, the resonant tunneling diodes in oscillating circuits can be used for strain detection and therefore as sensing elements [14].

In the recent work, we fall back on the strongly pronounced nonlinear current-voltage characteristics of a tunnel diode, and therewith associated multiple equilibria, correspondingly, nontrivial trajectories in the state-space. Due to its negative differential resistance, the diode's non-linear characteristic has two stable operating points with the same current response, cf. Fig. 1. This characteristic combined, with standard diode behavior as ultra-fast heterostructure device, allows it to be used in circuits as a storage element with bistable output voltage, *low* and *high*, and fast switching transients between both. Switching between the two states can be accomplished by the pulse signal added to a necessary voltage offset (bias). Such a nonlinear circuit with tunnel diode and output voltage to be controlled is used in our study, while representing a reach-on-dynamics nonlinear control system with hybrid, i.e. mixed time-continuous and discrete, behavior. Recall that the hybrid systems are ubiquitous and we see and interact with them on a daily basis [6], [11], [12]. Therefore, the objective of this paper is an experimental design and analysis of the nonlinear circuit, based on the tunnel diode, which can later on serve for investigation and verification of various hybrid control strategies, with particular focus on stability, reachability, and computational efficiency.

The paper is organized as follows: In Section II, we summarize the modeling of the nonlinear circuit with the tunnel diode. Following, the designed and assembled circuit with measuring and controlling devices are described in Section III. The experimental identification of diode characteristics is shown in Section IV. The analysis of transient response circuits behavior is provided in Section V. A simple open loop switching control of bistable output voltage is demonstrated with experiments in Section VI. Finally, Section VII summarizes the paper and gives brief outlook on the future works.

II. Modeling of non-linear Circuit

The system under consideration is based on an electric circuit using a tunnel diode as a non-linear component. The idea for this nonlinear system is inspired by a classical example from Khalil [10]. Besides the tunnel diode, the energy storage elements, i.e. capacitor and inductance, are also involved, equally as a resistive element and a voltage source.

In order to analyze and allow for numerical simulation of the circuit, the following differential equations are assumed first. Seeing the capacitance and the inductance to be time-invariant and linear we can write

$$i_C = C\frac{dv_C}{dt}, \quad v_L = L\frac{di_L}{dt}, \tag{1}$$

where i and v represent the current and, respectively, the voltage across the components. The subscript describes which component is referred to, while C and L represent the components. For the state model we define state x_1 as the voltage across the diode v_R, and state x_2 as the current through the inductance i_L. Furthermore the controllable input voltage is

TABLE I
INITIAL COMPONENTS CONFIGURATION

Components	Reference values [10]	Experimental values
R	1.5kΩ	1.5kΩ
C	2pF	12pF
L	5μH	4.7μH

given by u. In order to get a state equation for x_1, i_C has to be expressed as a function of the state variables x_1, x_2, and input u.

Applying the first of Kirchoff's law at the intersection point, meaning that the sum of all currents must be equal to zero, we obtain the following equation

$$i_R = i_C + i_L. \tag{2}$$

Further, knowing that the characteristic of the tunnel diode is a function of x_1, we can rewrite (2) to

$$i_C = -h(x_1) + x_2. \tag{3}$$

Also v_L should be described as a function of state variables x_1,x_2 and input u. Applying Kichoff's second law, meaning that all voltages in a closed pathway must be equal to zero, we can write

$$E = Ri_L + v_L + v_c, \tag{4}$$

while the total potential difference is set to be the input control value, i.e. $E = u$. Therefore, we obtain

$$v_L = -x_1 - Rx_2 + u. \tag{5}$$

Now v_L and i_C from (1) can be substituted by (3) and (5) which results in the two state equations

$$\dot{x}_1 = \frac{1}{C}[-h(x_1) + x_2], \tag{6}$$

$$\dot{x}_2 = \frac{1}{L}[-x_1 - Rx_2 + u]. \tag{7}$$

For further reference, the state x_2 will be referred to as u_D instead of u_R, since the voltage across the diode is an output value of interest. Using both state equations, a nonlinear state model can be directly implemented for numerical simulations.

III. TEST SETUP AND EXPERIMENT

The experimental test setup corresponds to the circuit provided in [10]. For hardware assembly, the components with values different from those assumed in [10] where used, due to the parts in stock, cf. Table I.

For the diode element, a vintage tunnel diode from General Electric, Type 1N3716 has been used [4]. A typical static curve with most relevant characteristic points for a chosen diode can be seen in Fig. 1 and Table II.

The circuit is set up on a universal interface bread board. As a measurement and control interface for the electric circuit, a dSpace MicroLabBox has been used [3]. To connect the MicroLabBox to the circuit, standard BNC connectors are used. The output ports of the MicroLabBox provide $\pm 10V$

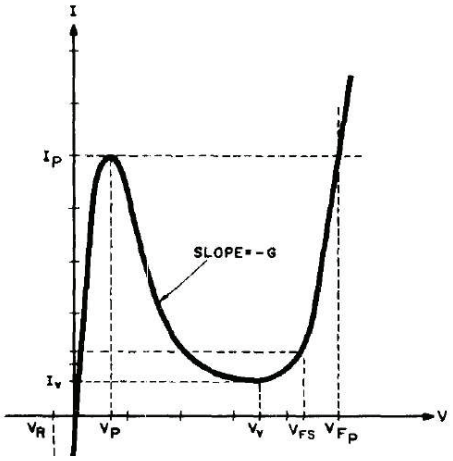

Fig. 1. Typical characteristic curve of tunnel diode [4]

TABLE II
DIODE CHARACTERISTIC POINTS [4]

Static Characteristics	Symbol	Value
Peak Point Current	I_P	4.7mA
Valley Point Current	I_V	0.6mA
Peak Point Voltage	V_P	65mV
Valley Point Voltage	V_V	350mV
Forward Voltage	V_{FP}	500mV

with a current range of $\pm 8mA$ and an offset error of $\pm 4mV$. The settling time is given with $1\mu s$ and the resolution of A/D conversion is 16bit. The board channels have also a circuit protecting them from over-voltage or -current.

The analogue out-port is the input voltage to the circuit representing u in (7). The voltage to drive the circuit is directly supplied by the analogue output channel. Although the current provided from the MicroLabBox would be enough for the diode only, the rest of the circuit should be additionally energized. Therefore an operational amplifiers (OP) of type LM324AN [8] has been used to boost the maximum available current up to $30mA$. The OP is in voltage follower configuration without any gain, having the same output voltage as the input.

On the input side of the MicroLabBox, the measuring input channels have the voltage range of $\pm 11V$, with a resolution of 16bit and a sampling rate of $10^6 Hz$, i.e. $1\mu s$ sampling time. For measurements, three BNC cables where connected to the circuit. One to measure u, another one – across a shunt resistor of 1Ω – to measure the state x_2, which is the inductor current i_L. The last one is directly connected across the diode, for measuring the state x_1, corresponding to u_D output. Thus, the electric diagram of the implemented setup is shown in Fig. 2, where the points of measuring are indicated with the symbols $\textcircled{M_x}$. Respectively, the experimental setup in the room temperature environment is shown on the picture in Fig. 3.

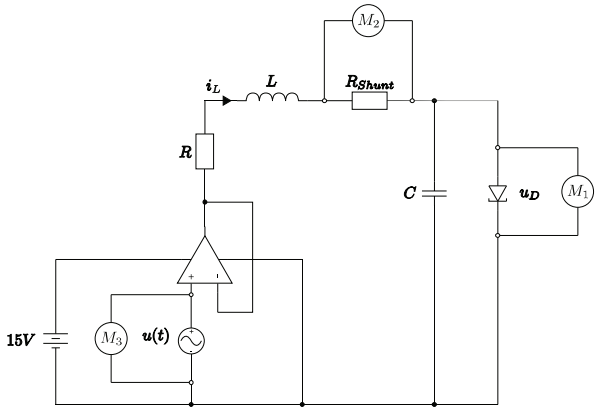

Fig. 2. Electrical diagram for experimental setup of complete circuit

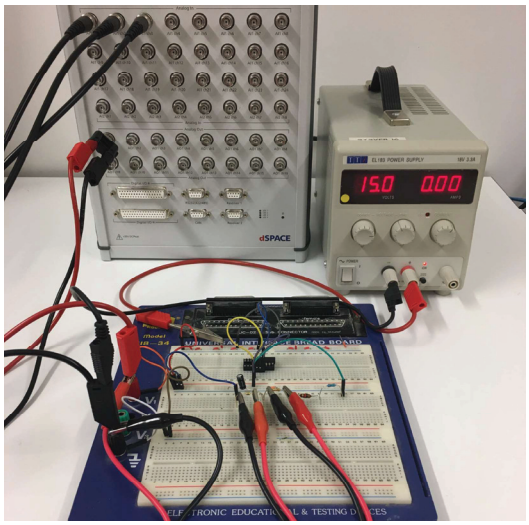

Fig. 3. Experimental setup

IV. Measuring of Diode Characteristic

For reliable modeling and numerical simulation of the circuit, the actual characteristic of the diode had to be determined from measurements. For that, R, L, and C shown in Fig. 2 have been first taken out, and a sinusoidal voltage was supplied to u in a closed-loop configuration, with a feedback integrator only. The current, via a shunt resistor added in front of the diode, and the voltage across the diode have been measured. The feedback integrator has been used in order to ensure that the diode's voltage follows the input voltage closely. Multiple measurements where taken, with the configuration values shown in Table III.

For each of the listed configurations, 10 measurements were performed at different times, with 10 periods each. Trigger conditions for measurement recording was set to 0.4V rising flank for the voltage across the diode. The following diagrams show one exemplary measurement, corresponding to *M.2* configuration as in Table III. The raw measurement data couldn't be used for identification, as it turns out the

TABLE III
Configuration of diode characteristic measurement values

Configuration	M.1	M.2	M.3
Sine amplitude	0.25V	0.25V	0.25V
Sine offset	0.25V	0.25V	0.25V
Sine frequency	5Hz	10Hz	100Hz
Integrator	100	100	5000

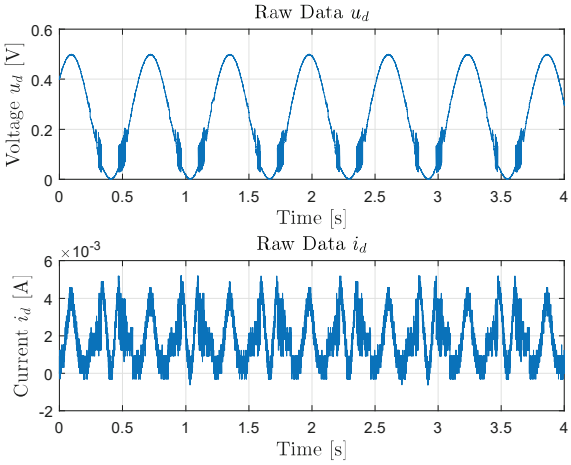

Fig. 4. Diode characteristic - raw voltage and current measurement

signal of the diode's voltage seems to be rather smooth while the current measurement included non-neglectable noise, see Fig. 4. Trying to boost the signal of the current measurement, using an instrumentation amplifier, appears less useful due to a low signal to noise ratio of the signal. Therefore, a Fast Fourier Transformation (FFT) has been first performed on both the current and voltage measurements, see Fig. 5. It can be seen that while, the power spectrum of the measured

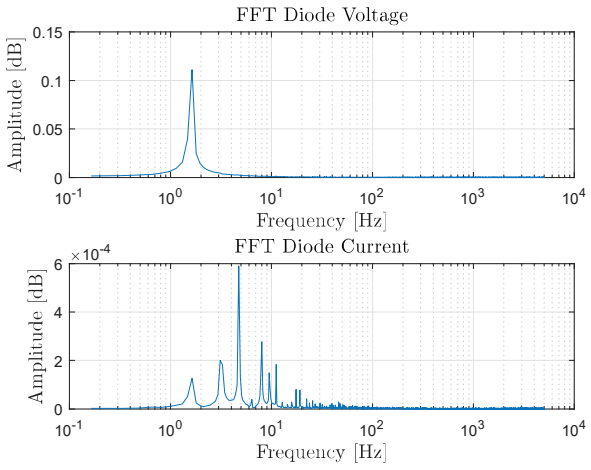

Fig. 5. Diode characteristic - FFT

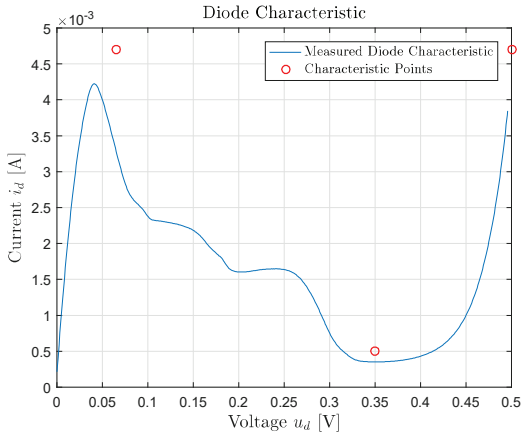

Fig. 6. Diode characteristic curve with characteristic points from data sheet

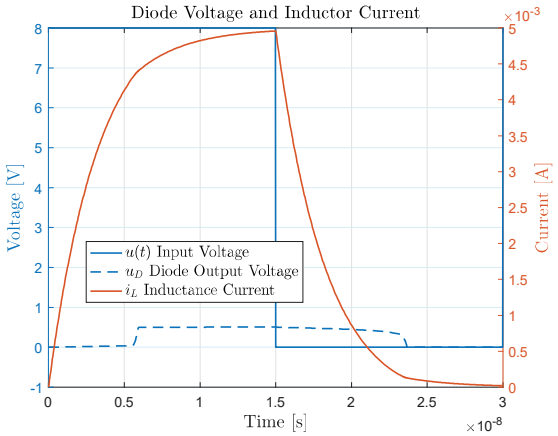

Fig. 7. Transient response of diode, numeric simulation as in Table I

voltage disclose the one principal harmonic, the spectrum distrusting of the measured diode current clearly demonstrate multiple frequency components right-hand side to the principal harmonic. This is supposedly due to inherently nonlinear nature of the tunnel diode, though will not be further analyzed, correspondingly discussed, due to a different focus of the recent work. Afterwards, a low pass filter has been applied, resulting in a more smooth measured characteristic. Also, the filtered data was cropped to full periods so as to avoid the initial "bending" of signals due to the filtering.

Next, all data points within a moving frame of $1mV$, were averaged for the voltage and current signal, thus giving a data point every $1mV$ within the range of 0 to $0.5V$. Finally, the obtained characteristic points have been shifted to start at $0V$ and, if necessary, smoothened out using a moving average. Note hat the shift of zero voltage is reasonably required since the shunt, connected in series, provided an additional low voltage drop which is not belonging to diode's characteristic. The settings applied for filtering and smoothing the data from the chosen configuration M.2 are as follows: filter order 2^9 and cutoff frequency $30Hz$.

After evaluating all measurements in the same manner, we came to the conclusion, that the determined (final) characteristic from the measurements with M.2 configuration are closest to the generalized characteristic curve and nominal (manufacturer provided) data points. The final characteristic curve, as well as the characteristic points from the data sheet II, are shown in Fig. 6. Further it can be noted that the data spread of the 10 repeated measurements has been equally evaluated and yielded negligible.

V. Transient Response and Circuit Analysis

Performing a numerical simulation when applying a pulse signal at the system u, we see the state response as shown in Fig. 7. Here, the parameter reference values as in Table I, have been used in order to analyze the circuits behavior. From the open loop response it can be recognized, that the time constants are relatively short and are in the region of

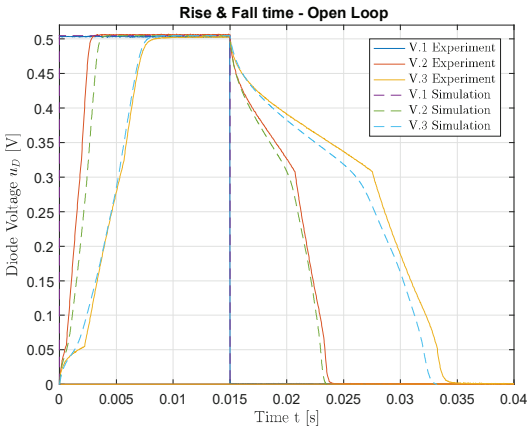

Fig. 8. Simulation and experiment response according to Table IV

a few nano-seconds. Therefore, initial circuits configuration is significantly faster than available sampling time of the MicroLabBox controller. Therefore, the circuits time response is required to be slower than about $100\mu s$, so as to allow for sufficient sampling during the transient phases. Different values for the components C and L have been tried to alter the response time. The chosen values, based on components available, are shown in Table IV. The results of numerical simulation and experimental measurements are compared with each other in Fig. 8 for all three components' configurations. One can see, that for all three configurations, the measured response of the circuit is well in accord with the modeled one, in both steady-state and transient (rise time) phases. This argues in favor of the designed and identified system, and allows for using numerical simulation for future analysis in control strategies. For further experiments, the components' configuration *V.3* has been chosen as a sufficiently slow and, therefore, suitable for capturing the transient response.

Also, a frequency sweep has been simulated in order to check at which signal frequencies the corresponding response of the circuit is going to be affected. For the simulation, the

TABLE IV
COMPONENTS' CONFIGURATIONS

Component	V.1	V.2	V.3
R	1.5kΩ	1.5kΩ	1.5kΩ
C	12pF	22μF	47μF
L	4.7μH	1mH	1mH

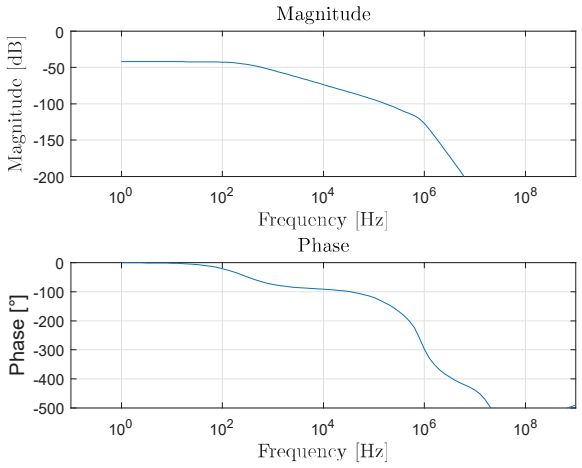

Fig. 9. Bode plot of the circuit

values of configuration *V.3* from Table IV have been assumed as well. From Fig. 9 one can see, that starting from about $100Hz$, a magnitude decrease is already observable. Also the phase starts decaying already at relatively low frequencies. Furthermore, it has to be mentioned that the numerical simulation has performed for a system model based on Fig. 2, therefore including the OP, supply voltage and measuring elements. The model for simulation was created using the National Instrument Multisim 14.0 which has the OP LM324AN in library. However, the exact diode used in our test setup was not available, and the next best match was taken in order to perform the simulation, i.e. a diode of type 1N3715 instead of 1N3716. Despite the dynamic system with only two integrators is expected to have the phase response converging to $-180°$, from Fig. 9 one can see that the phase goes far beyond $-180°$. This is mainly caused by high frequency behavior of LM324AN amplifier and possible impact of nonlinearities on the estimation of frequency response function.

Next, in order to analyze the fast (transient) switching between two bistable states, a sine signal with the frequency of $10Hz$, amplitude of $5V$, and offset of $5V$ was applied to the input of the circuit. The measured results are shown in Fig. 10, from which one can clearly see a two-level output state behavior, as hysteresis in the input-output voltage coordinates. Diode output voltages of less than $0.1V$ can be considered as *low* level, while the voltages above $0.4V$ can be considered as *high* level. Obviously, the designed circuit provides the expected memory effect due to the energy storage

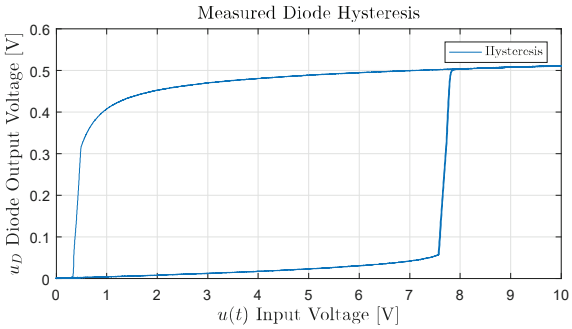

Fig. 10. Measured input-output hysteresis curve of diode

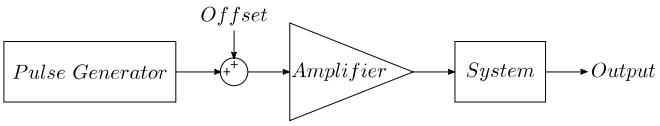

Fig. 11. Open loop control structure

in combination with nonlinear voltage-current characteristics of the tunnel diode.

VI. OPEN LOOP CONTROL

The open loop control setup, which the following measurements were taken from, is shown in Fig. 11. Varying configurations of pulse signals have been used. The goal is to switch between two bistable states, with a short pulse around the offset voltage, which value is $4.1V$. The configurations applied to the system are shown in Table V.

Taking a look at Fig. 12 one can see that both states are easily reached, when a pulse in positive or negative direction is applied over the offset. However, once we reduce the pulse-width to less than 19% (using 1% increments), the signal is not able to reach both states anymore which can be seen from Fig. 13. Interesting to mention is that although the output voltage reached almost its lower state, it bounces back up to the state *high* only due to the voltage of the offset.

Furthermore, coming back to a pulse-width of 32% but lowering the voltage gradually (using $0.1V$ increments), one can see that at the input voltage level of $3.4V$ the system is not able to switch between the two states anymore either, as can be seen in Fig 14. The same behavior, not being able to switch between states, can be observed in the *worst case scenario*, combining low voltage and and short pulse width, see Fig. 15.

TABLE V
AMPLITUDE, OFFSET AND PULSE-WIDTH SETTINGS FOR EXPERIMENTS AND CORRESPONDING FIGURE REFERENCES

	Amplitude $3.4V$ **Offset** $4.1V$	**Amplitude** $5V$ **Offset** $5V$
Pulsewidth 32%	Fig. 14	Fig. 12
Pulsewidth 18%	Fig. 15	Fig. 13

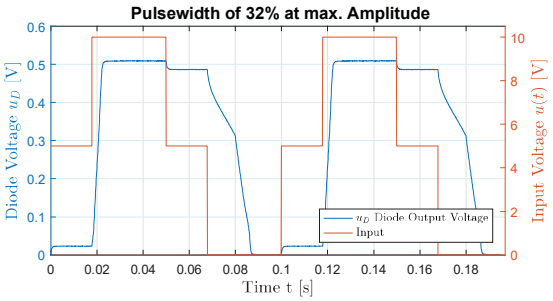

Fig. 12. Measured input voltage and system response at amplitude of $5V$, offset $5V$ with pulse-width of 32%

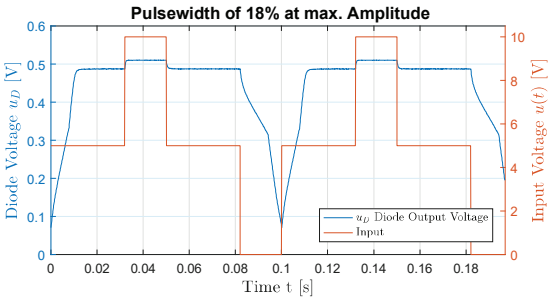

Fig. 13. Measured input voltage and system response at amplitude of $5V$, offset $5V$ with pulse-width of 18%

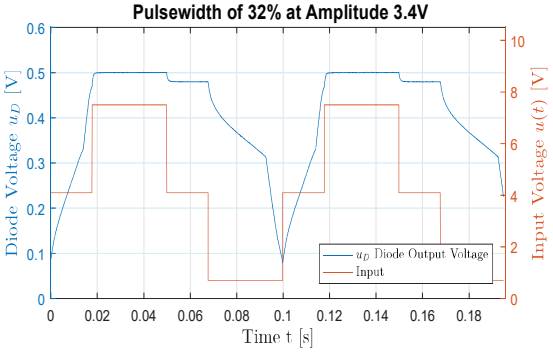

Fig. 14. Measured input voltage and system response at amplitude of $3.4V$, offset $4.2V$ with pulse-width of 32%

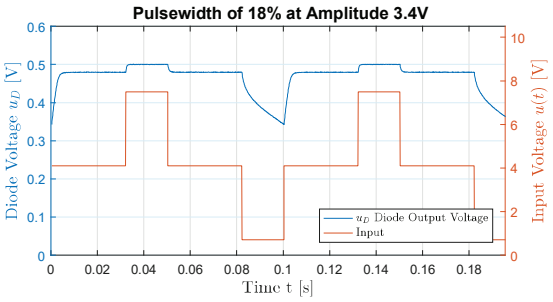

Fig. 15. Measured input voltage and system response at amplitude of $3.4V$, offset $4.2V$ with pulse-width of 18%

Therefore it can be concluded, that the minimum pulse-width at which the system is still able to switch between states *high* and *low* is depending on the systems input voltage provided and the pulsewidth, assuming that the offset voltage is in the middle of the hysteresis. On our test setup, one is limited to the maximal $10V$, therefore the maximum possible pulse amplitude to induce is $5V$.

VII. Summary and Outlook

In this work, the non-linear electric circuit with tunnel diode has been designed and implemented on an experimental setup. The classical model, known from literature [10], has been assumed, while the system parameters have been assumed from the data sheets of standard linear components and identified by series of dedicated experiments. The nonlinear characteristics of the tunnel diode have been determined from the measurements and compared with typical characteristic curves and the few characteristic points available from the components' documentation. Both, the steady-state and transient responses of the overall system have been analyzed based on experiments. Also, an open loop control with biased impulses have been realized and evaluated, allowing for a bistable output voltage behavior. The knowledge gained by conducting the simulations and experiments for this setup, now enables us to apply various hybrid control methods [11], [9] and perform a formal analysis [1], [5] for different tools designed for hybrid control verification. Having validated analysis tools to verify the proper function of the control scheme is therefore of utmost importance.

References

[1] Alur, R. Formal verification of hybrid systems. *Emsoft* (2011), 273—-278.

[2] Bergman, R. H. Tunnel diode logic circuits. *IRE Transactions on Electronic Computers*, 4 (1960), 430–438.

[3] dSpace. MicroLabBox - dSPACE, 2017.

[4] Elfa Distrelec. Tunnel Diodes, 2017.

[5] Fehnker, A., Fehnker, A., Ivancic, F., and Ivancic, F. Benchmarks for Hybrid Systems Verification. *Hybrid Systems: Computation and Control 15213* (2004), 326 – 341.

[6] Goebel, R., Sanfelice, R. G., and Teel, A. R. Hybrid dynamical systems. *IEEE Control Systems 29*, 2 (2009), 28–93.

[7] Hall, R. Tunnel diodes. *IRE Transactions on Electron Devices 7*, 1 (1960), 1–9.

[8] Instruments, T. LM324AN Texas Instruments — Mouser Germany, 2017.

[9] Johansson, K. H. Hybrid control systems.

[10] Khalil, H. *Nonlinear Systems*, 3rd ed. Prentice Hall, 2002.

[11] Lin, H., and Antsaklis, P. *Hybrid Dynamical Systems: An Introduction to Control and Verification*. Now Publishers, 2014.

[12] Lunze, J., and Lamnabhi-Lagarrigue, F. *Handbook of hybrid systems control: theory, tools, applications*. Cambridge University Press, 2009.

[13] Sommers, H. Tunnel Diodes as High-Frequency Devices. *Proceedings of the IRE 47*, 7 (1959), 1201–1206.

[14] Tajika, T., Kakutani, Y., Mori, M., and Maezawa, K. Experimental demonstration of strain detection using resonant tunneling delta-sigma modulation sensors. *Physica status solidi (a) 214*, 3 (2017), 1600548.